arXiv:cond-mat/0609594v1 [cond-mat.str-el] 25 Sep 2006

Kinks in the dispersion of strongly correlated electrons

K. Byczuk,[1, 2] M. Kollar,[1] K. Held,[3] Y.-F. Yang,[3] I. A. Nekrasov,[4] Th. Pruschke,[5] and D. Vollhardt[1]
[1] *Theoretical Physics III, Center for Electronic Correlations and Magnetism,*
Institute for Physics, University of Augsburg, 86135 Augsburg, Germany
[2] *Institute of Theoretical Physics, Warsaw University, ul. Hoża 69, PL-00-681 Warszawa, Poland*
[3] *Max-Planck Institute for Solid State Research, Heisenbergstr. 1, 70569 Stuttgart, Germany*
[4] *Institute for Electrophysics, Russian Academy of Sciences, Ekaterinburg, 620016, Russia*
[5] *Institute for Theoretical Physics, University of Göttingen,*
Friedrich-Hund-Platz 1, 37077 Göttingen, Germany

(22-Sep-2006)

The properties of condensed matter are determined by single-particle and collective excitations and their interactions. These quantum-mechanical excitations are characterized by an energy E and a momentum $\hbar \boldsymbol{k}$ which are related through their *dispersion* $E_{\boldsymbol{k}}$. The coupling of two excitations may lead to abrupt changes (*kinks*) in the slope of the dispersion. Such kinks thus carry important information about interactions in a many-body system. For example, kinks detected at 40-70 meV below the Fermi level in the electronic dispersion of high-temperature superconductors are taken as evidence for phonon [1, 2] or spin-fluctuation based [3, 4] pairing mechanisms. Kinks in the electronic dispersion at binding energies ranging from 30 to 800 meV are also found in various other metals [5, 6, 7, 8, 9, 10, 11, 12, 13, 14, 15, 16, 17] posing questions about their origins. Here we report a novel, purely electronic mechanism yielding kinks in the electron dispersions. It applies to strongly correlated metals whose spectral function shows well separated Hubbard subbands and central peak as, for example, in transition metal-oxides. The position of the kinks and the energy range of validity of Fermi-liquid (FL) theory is determined solely by the FL renormalization factor and the bare, uncorrelated band structure. Angle-resolved photoemission spectroscopy (ARPES) experiments at binding energies outside the FL regime can thus provide new, previously unexpected information about strongly correlated electronic systems.

In systems with a strong electron-phonon coupling kinks in the electronic dispersion at 40–60 meV are well known [5, 6, 7]. Collective excitations other than phonons, or even an altogether different mechanism, may be the origin of kinks detected at 40 meV in the dispersion of surface states of Ni(110) [8]. Surface states of ferromagnetic Fe(110) show similar kinks at 100-200 meV [9], and even at 300 meV in Pt(110) – far beyond any phononic energy scale [10]. Kinks at unusually high energies are also found in transition-metal oxides [11, 12, 13, 14, 15], where the Coulomb interaction leads to strong correlations, e.g., at 150 meV in $SrVO_3$ [16]. Unexpectedly, kinks at 380 meV and 800 meV were reported recently for three different families of high-temperature superconductors at different doping levels [17].

Interactions between electrons or their coupling to other degrees of freedom change the notion of $E_{\boldsymbol{k}}$ as the energy of an isolated electron or of a mode with infinite lifetime. Namely, the interactions lead to a damping effect implying that the dispersion relation is no longer a real function. For systems with Coulomb interaction FL theory predicts the existence of fermionic quasiparticles [18], i.e., exact one-particle states with momentum $\boldsymbol{k}$ and a real dispersion $E_{\boldsymbol{k}}$, at the Fermi surface and at zero temperature. This concept can be extended to $\boldsymbol{k}$ states sufficiently close to the Fermi surface (*low-energy regime*) and at low enough temperatures, in which case the lifetime is now finite but still long enough for quasiparticles to be used as a concept.

Outside the FL regime the notion of dispersive quasiparticles is, in principle, inapplicable since the lifetime of excitations is too short. However, it is an experimental fact that $\boldsymbol{k}$-resolved one-particle spectral functions measured by ARPES often show distinct peaks also at energies far away from the Fermi surface. The positions of those peaks change with $\boldsymbol{k}$, which means that the corresponding one-particle excitations are *dispersive*, in spite of their rather short lifetime. It turns out that kinks in the dispersion relation are found in this energy region outside the FL regime [1, 2, 3, 4, 5, 6, 7, 8, 9, 10, 11, 12, 13, 14, 15, 16, 17].

We describe here a novel mechanism leading to kinks in the dispersion of strongly correlated electrons, which does not require any coupling to phonons or other excitations. To set the stage for this mechanism, which requires strong correlations, we consider first a weakly correlated system. Imagine we inject an electron into the partially filled band at an energy close to the Fermi surface. In this process the entire system becomes excited, leading to the generation of many quasiparticles and -holes. In view of their long lifetime the Coulomb interaction with other quasiparticles or -holes modifies their dispersion which, according to FL theory, becomes $E_{\mathbf{k}} = Z_{\mathrm{FL}}\epsilon_{\boldsymbol{k}}$. Here Z_{FL} is a FL renormalization factor and $\epsilon_{\boldsymbol{k}}$ is the

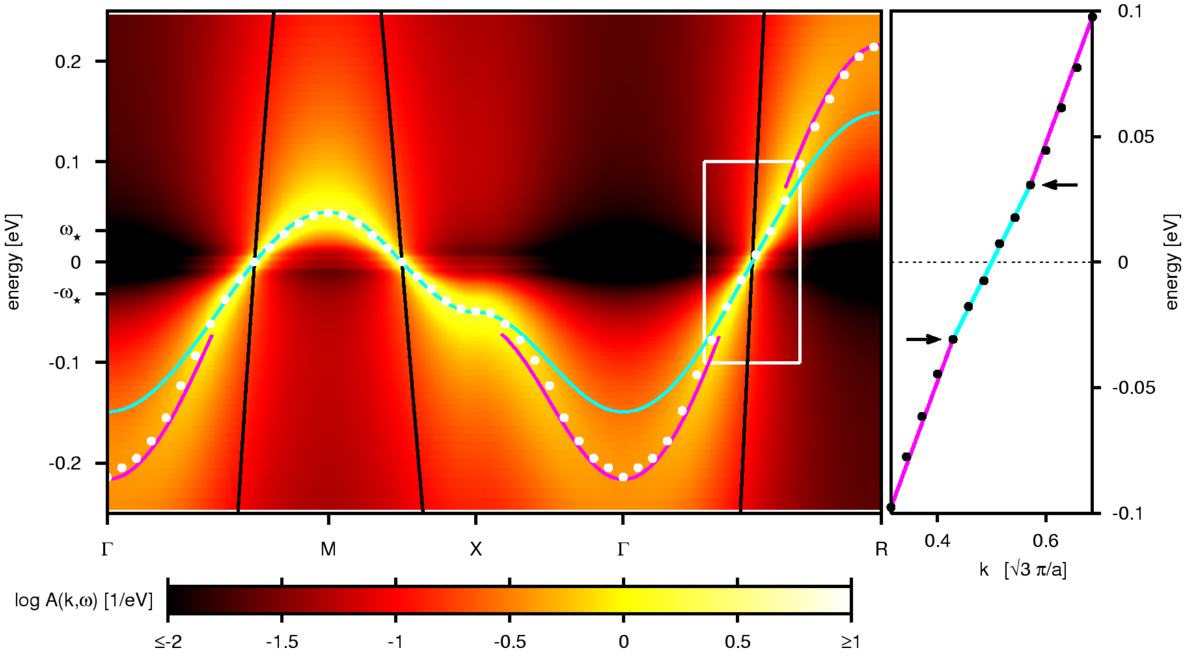

FIG. 1: **Kinks in the dispersion relation $E_{\boldsymbol{k}}$ for a strongly correlated system**. The intensity plot represents the spectral function $A(\boldsymbol{k},\omega)$ (Hubbard model in DMFT, cubic lattice, interaction U=3.5 eV, bandwidth $W \approx$ 3.64 eV, n=1, $Z_{\rm FL}$=0.086, $T = 5$ K). Close to the Fermi energy the effective dispersion (white dots) follows the renormalized band structure $E_{\boldsymbol{k}} = Z_{\rm FL}\epsilon_{\boldsymbol{k}}$ (blue line). For $|\omega| > \omega_\star$ the dispersion has the same shape but with a different renormalization, $E_{\boldsymbol{k}} = Z_{\rm CP}\epsilon_{\boldsymbol{k}} - c\ \mathrm{sgn}(E_{\boldsymbol{k}})$ (pink line). Here $\omega_\star$=0.03 eV, $Z_{\rm CP} = 0.135$, and $c = 0.018$ eV are all calculated (see appendix) from $Z_{\rm FL}$ and $\epsilon_{\boldsymbol{k}}$ (black line). A subinterval of Γ-R (white frame) is plotted on the right, showing kinks at $\pm\omega_\star$ (arrows).

bare (noninteracting) dispersion. By contrast, an electron injected at an energy far from the Fermi level leads to excitations with only a short lifetime; their dispersion is hardly affected by the weak interaction, i.e., $E_{\boldsymbol{k}} \approx \epsilon_{\boldsymbol{k}}$ (see appendix). The crossover from the FL dispersion to the noninteracting dispersion can lead to kinks near the band edges which mark the termination point of the FL regime. However, for weakly correlated metals ($Z_{\rm FL} \lesssim 1$) the slope of $E_{\boldsymbol{k}}$ changes only a little; hence the kinks are not very pronounced.

The situation is very different in strongly correlated metals where $Z_{\rm FL}$ can be quite small such that kinks can be well-pronounced. The strong interaction produces a strong redistribution of the spectral weight in the one-particle spectral function. Namely, the conducting band develops so-called Hubbard subbands, whose positions are determined by the atomic energies. For metallic systems a resonant central peak emerges around the Fermi level which lies between these subbands. The central peak of this so-called three-peak structure is often interpreted as a “quasiparticle peak”, but it will be shown below that genuine FL quasiparticles exist only in a *narrow* energy range around the Fermi level. Outside this FL regime, but still inside the central peak, we identify a new *intermediate-energy* regime, where the dispersion is given by $E_{\mathbf{k}} \approx Z_{\rm CP}\epsilon_{\boldsymbol{k}}$. Here $Z_{\rm CP}$ is a new renormalization factor, given by the weight of the *c*entral *p*eak, which differs significantly from $Z_{\rm FL}$. At these intermediate energies, which are much smaller than the interaction strength, an injected electron or hole is still substantially affected by the other electrons in the system. Therefore its dispersion is neither that of a free system, nor that of the (strongly renormalized) FL regime, but rather corresponds to a *moderately* correlated system ($Z_{\rm FL} < Z_{\rm CP} < 1$). As a consequence there occurs a crossover at an intermediate energy $\pm\omega_\star$ inside the central peak from $Z_{\rm FL}$ renormalization to $Z_{\rm CP}$ renormalization, which is visible as kinks in the dispersion. As shown below, in a microscopic theory the position of those kinks and the breakdown of the FL regime are directly related. We emphasize that this mechanism yields kinks but does not involve coupling of electrons and collective modes; only strong correlations between electrons are required.

For a microscopic description of these electronic kinks we use the Hubbard model, which is the generic model for strongly correlated electrons, and solve it by many-body dynamical mean-field theory (DMFT) [19, 20, 21, 22], using the numerical renormalization group as an impurity solver. We focus on a single band with particle-hole symmetry and discuss the asymmetric case in the appendix. For the strongly correlated Hubbard model (interaction $U \approx$ bandwidth) the dispersion relation is shown in Fig. 1

and the spectral function in Fig. 2a. The dispersion relation $E_{\boldsymbol{k}}$ crosses over from the Fermi-liquid regime (blue line in Fig. 1) to the intermediate-energy regime (pink line in Fig. 1), as described above, and shows pronounced kinks at the energy scale $\omega_\star = 0.03$ eV. In some directions in the Brillouin zone these kinks may be less visible because the band structure is flat (e.g., near the X point in Fig. 1). The behavior of $E_{\boldsymbol{k}}$ is now analyzed quantitatively.

The physical quantity describing properties of one-particle excitations in a many-body system is the Green function or "propagator" $G(\boldsymbol{k}, \omega) = (\omega + \mu - \epsilon_{\boldsymbol{k}} - \Sigma(\boldsymbol{k}, \omega))^{-1}$, which characterizes the propagation of an electron in the solid [18]. Here ω is the frequency, μ the chemical potential, $\epsilon_{\boldsymbol{k}}$ the bare dispersion relation, and $\Sigma(\boldsymbol{k}, \omega)$ is the self-energy, a generally complex quantity describing the influence of interactions on the propagation of the one-particle excitation, which vanishes in a noninteracting system. The effective dispersion relation $E_{\boldsymbol{k}}$ of the one-particle excitation is determined by the singularities of $G(\boldsymbol{k}, \omega)$, which give rise to peaks in the spectral function $A(\boldsymbol{k}, \omega) = -\mathrm{Im}G(\boldsymbol{k}, \omega)/\pi$. If the damping given by the imaginary part of $\Sigma(\boldsymbol{k}, \omega)$ is not too large, the effective dispersion is thus determined by $E_{\boldsymbol{k}} + \mu - \epsilon_{\boldsymbol{k}} - \mathrm{Re}\Sigma(\boldsymbol{k}, E_{\boldsymbol{k}}) = 0$. Any kinks in $E_{\boldsymbol{k}}$ that do not originate from $\epsilon_{\boldsymbol{k}}$ must therefore be due to slope changes in $\mathrm{Re}\Sigma(\boldsymbol{k}, \omega)$.

In many three-dimensional physical systems the $\boldsymbol{k}$ dependence of the self-energy is less important than the ω dependence and can be neglected to a good approximation. Then one may use the DMFT self-consistency equations to express $\Sigma(\boldsymbol{k}, \omega) = \Sigma(\omega)$ as $\Sigma(\omega) = \omega + \mu - 1/G(\omega) - \Delta(G(\omega))$, where $G(\omega) = \int G(\boldsymbol{k}, \omega)\, d\boldsymbol{k}$ is the local Green function (averaged over $\boldsymbol{k}$) and $\Delta(G)$ is an energy-dependent hybridization function, expressed here as a function of $G(\omega)$ [23]. The hybridization function describes how the electron at a given lattice site is quantum-mechanically coupled to the other sites in the system. It plays the role of a dynamical mean-field parameter and its behavior is strongly dependent on the electronic correlations in the system. Fig. 2a shows a typical result for the integrated spectral function $A(\omega) = -\mathrm{Im}G(\omega)/\pi$ with the aforementioned three-peak structure. The corresponding real parts of the local propagator $G(\omega)$ and self-energy $\Sigma(\omega)$ are shown in Fig. 2b and Fig. 2c, respectively.

Kinks in $\mathrm{Re}\Sigma(\omega)$ appear at a new small energy scale which emerges quite generally for a three-peak spectral function $A(\omega)$. Kramers-Kronig relations imply that $\mathrm{Re}[G(\omega)]$ is small near the dips of $A(\omega)$, located at $\pm\Omega$. Therefore $\mathrm{Re}[G(\omega)]$ has a maximum and a minimum at $\pm\omega_{\max}$ *inside the central spectral peak* (Fig. 2b). This directly leads to kinks in $\mathrm{Re}\Sigma(\omega)$ for the following reason. There are two contributions to $\Sigma(\omega)$: $\omega + \mu - 1/G(\omega)$ and $-\Delta(G(\omega))$. While $\mathrm{Re}[\omega + \mu - 1/G(\omega)]$ is *linear* in the large energy window $|\omega| < \Omega$ (Fig. 2d), the term $-\mathrm{Re}[\Delta(G(\omega))]$ is approximately proportional to $-\mathrm{Re}[G(\omega)]$ (at least to first order in a moment expansion), and thus remains linear only in a much narrower energy window $|\omega| < \omega_{\max}$. The sum of these two contributions produces pronounced kinks in the real part of the self-energy at $\pm\omega_\star$, where $\omega_\star = (\sqrt{2} - 1)\omega_{\max}$ is the energy where $\mathrm{Re}[G(\omega)]$ has maximum curvature (marked by blue circles in Fig. 2c). The Fermi-liquid regime with slope $\partial\mathrm{Re}\Sigma(\omega)/\partial\omega = 1 - 1/Z_{\mathrm{FL}}$ thus extends only throughout a small part of the central peak ($|\omega| < \omega_\star$). At intermediate energies ($\omega_\star < |\omega| < \Omega$)

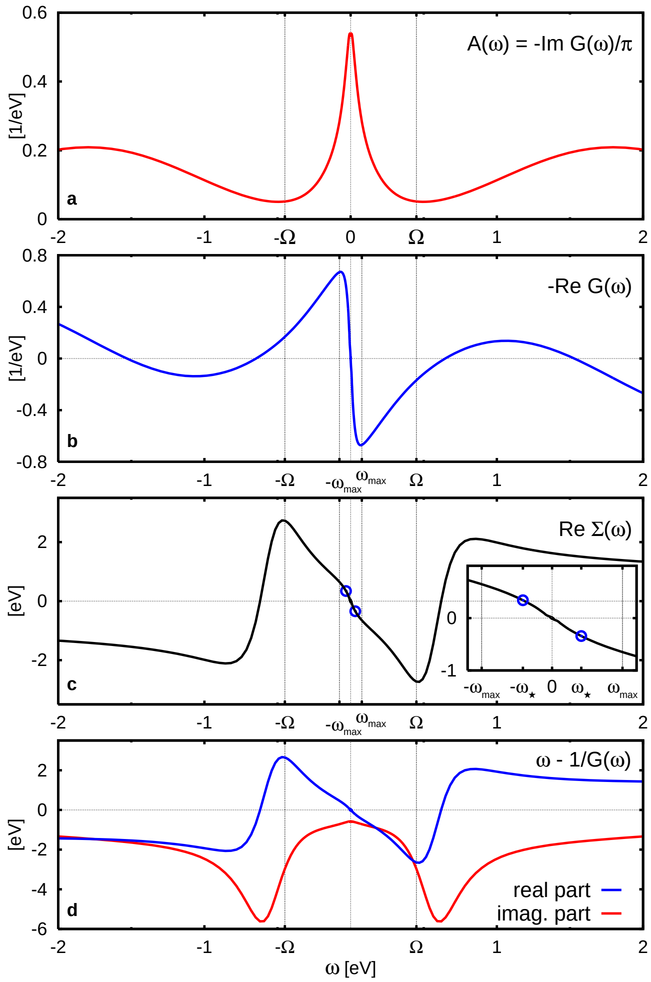

FIG. 2: **Local propagator and self-energy for a strongly correlated system (parameters as Fig. 1).** **a**, Correlation-induced three-peak spectral function $A(\omega) = -\mathrm{Im}G(\omega)/\pi$ with dips at $\pm\Omega = 0.45$ eV. **b**, Corresponding real part of the propagator, $-\mathrm{Re}G(\omega)$, with minimum and maximum at $\pm\omega_{\max}$ inside the central spectral peak. **c**, Real part of the self-energy with kinks at $\pm\omega_\star$ (blue circles), located at the points of maximum curvature of $\mathrm{Re}G(\omega)$, ($\omega_\star = 0.4\omega_{\max} = 0.03$ eV). **d**, $\omega - 1/G(\omega)$ contributes to the self-energy. In general $\mathrm{Re}[\omega - 1/G(\omega)]$ (blue line) is linear in $|\omega| < \Omega$. The other contribution to the self-energy is $-\Delta(G(\omega)) \approx -(m_2 - m_1^2)G(\omega)$ (to lowest order in the moments m_i of $\epsilon_{\boldsymbol{k}}$; here $m_2 - m_1^2$=0.5 eV^2). Therefore the nonlinearity of $-\mathrm{Re}[G(\omega)]$ at $\pm\omega_\star$ determines the location of kinks.

the slope is then given by $\partial \text{Re}\Sigma(\omega)/\partial\omega = 1 - 1/Z_{\text{CP}}$. The kinks at $\pm\omega_\star$ mark the crossover between these two slopes. As a consequence there is also a kink at $\omega_\star$ in the effective band structure $E_{\boldsymbol{k}}$.

The above analysis also explains why outside the FL regime $E_{\boldsymbol{k}}$ still follows the uncorrelated dispersion, albeit with a different renormalization Z_{CP} and a small offset c. This behavior is due to $\omega + \mu - 1/G(\omega)$, the main contribution to the self-energy inside the central peak for $\omega_\star < |\omega| < \Omega$. In particular our analysis explains the dependence of $E_{\boldsymbol{k}}$ on $\boldsymbol{k}$ that was observed in previous DMFT studies of SrVO_3 [24] (see appendix).

The FL regime terminates at the kink energy scale $\omega_\star$, which cannot be determined within FL theory itself. The quantities $\omega_\star$, Z_{CP}, and c can nevertheless all be expressed in terms of Z_{FL} and the bare density of states alone; explicitly, one finds $\omega_\star = Z_{\text{FL}}(\sqrt{2}-1)D$, where D is an energy scale of the noninteracting system, e.g., D is approximately given by half the bandwidth (see appendixfor details). For weak correlations ($Z_{\text{FL}} \lesssim 1$) the kinks in $E_{\boldsymbol{k}}$ thus merge with the band edges and are almost undetectable, as discussed above. On the other hand, for increasingly stronger correlations ($Z_{\text{FL}} \ll 1$) the kinks at $\omega_\star/D \propto Z_{\text{FL}}$ move closer to the Fermi energy and deeper inside the central peak, whose width diminishes only as $\Omega/D \propto \sqrt{Z_{\text{FL}}}$ [25].

The energy scale $\omega_\star$ involves only the bare band structure which can be obtained, for example, from band structure calculations, and the FL renormalization $Z_{\text{FL}} = 1/(1 - \partial\text{Re}\Sigma(0)/\partial\omega) \equiv m/m^*$ known from, e.g., specific heat measurements or many-body calculations. We note that since phonons are not involved in this mechanism, $\omega_\star$ shows no isotope effect. For strongly interacting systems, in particular close to a metal-insulator transition [22], $\omega_\star$ can become quite small, e.g., smaller than the Debye energy.

An analysis similar to the one presented above also holds for systems with strong hybridization such as the high-temperature superconductors, where the overlap between d and oxygen p states is important [26]. The assumption of a $\boldsymbol{k}$-independent self-energy may also be relaxed: if a correlation-induced three-peak spectral function $A(\boldsymbol{k},\omega)$ is present for a certain range of momenta $\boldsymbol{k}$, the corresponding self-energies $\Sigma(\boldsymbol{k},\omega)$ and effective dispersion $E_{\boldsymbol{k}}$ will also develop kinks, as can be proved using cluster extensions to DMFT.

In conclusion, we showed that kinks in the electronic dispersion result from strong correlations alone, i.e., even without coupling to collective modes such as phonons. The energy of these kinks is a quantitative measure of electronic correlations in many-body systems; it marks the termination point of the Fermi liquid regime and can be as high as several hundred meV. These kinks are a fingerprint of a strongly correlated metal and are expected to be observable in many materials, including high-temperature superconductors.

We acknowledge discussions with V. I. Anisimov, R. Bulla, J. Fink, A. Fujimori, and D. Manske. This work was supported by Deutsche Forschungsgemeinschaft through Sonderforschungsbereiche 484 (K.B., M.K., D.V.) and 602 (T.P.) and the Emmy-Noether program (K.H.), and in part by the Russian Basic Research foundation grants 05-02-16301, 05-02-17244, 06-02-90537 as well as by the RAS Programs *Quantum macrophysics* and *Strongly correlated electrons in semiconductors, metals, superconductors and magnetic materials*, Dynasty Foundation, Grant of President of Russia MK-2118.2005.02, interdisciplinary grant UB-SB RAS (I.N.). We thank the John von Neumann Institute for Computing, Forschungszentrum Jülich, and the Norddeutsche Verbund für Hoch- und Höchstleistungsrechnen for computing time.

APPENDIX: TECHNICAL DETAILS

Existence of kinks in the self-energy

A sufficient condition for kinks in the real part of the self-energy $\Sigma(\omega)$ and in the effective dispersion $E_{\boldsymbol{k}}$ is the existence of a correlation-induced three-peak structure in the spectral function $A(\omega) = -\text{Im}G(\omega)/\pi$. These kinks are located at energies inside the central peak of $A(\omega)$. This can be derived from the DMFT self-consistency condition,

$$\Sigma(\omega) = \omega + \mu - 1/G(\omega) - \Delta(G(\omega))\,, \qquad (1)$$

where $G(\omega)$ is the local Green function and $\Delta(G)$ is the hybridization function [23].

Suppose that $A(\omega)$ has three well-developed peaks with dips at $\Omega_\pm$ (Fig. 2a), i.e., the central peak is located in the interval $\Omega_- < \omega < \Omega_+$ (allowing for a general, asymmetric case). Kramers-Kronig relations imply that $\text{Re}G(\omega)$ becomes small in the vicinity of $\Omega_\pm$ and thus has extrema inside the central spectral peak (Fig. 2b). Consider now the complex function $\omega - 1/G(\omega)$. Peaks and dips in $A(\omega)$ are reflected as dips and peaks in $\text{Im}[-1/G(\omega)]$, respectively (red line in Fig. 2d). By Kramers-Kronig relations, the peaks of $\text{Im}[-1/G(\omega)]$ near $\Omega_\pm$ imply zeros in $\omega - \text{Re}[1/G(\omega)]$, which thus has one maximum and one minimum inside the central peak (blue line in Fig. 2d). Hence we find that *inside the central peak* $\text{Re}[\omega - 1/G(\omega)]$ *is monotonous and may be approximated by a straight line*, provided $A(\omega)$ is sufficiently smooth. Thus there are two different contributions to $\text{Re}\Sigma(\omega)$ (Fig. 2c): (i) $\text{Re}[\omega + \mu - 1/G(\omega)]$ is approximately linear in ω throughout the central spectral peak, while (ii) $\text{Re}[-\Delta(G(\omega))]$ is linear in a smaller interval $\omega_{\star,-} < \omega < \omega_{\star,+}$, thus *leading to kinks in* $\text{Re}\Sigma(\omega)$ *inside the central spectral peak.* Below we determine the location $\omega_{\star,\pm}$ of these kinks and the resulting effective dispersion relation $E_{\boldsymbol{k}}$.

Location of kinks in the self-energy

As discussed above, since $\mathrm{Re}[\omega+\mu-1/G(\omega)]$ is approximately linear in this interval, we can expand the inverse of the local propagator as $1/G(\omega) = z_0 + z_1\omega + O(\omega^2)$ for small ω. We rewrite this as

$$G(\omega) = \frac{Z_{\mathrm{CP}}}{\omega - \omega_0 + i(\gamma + \gamma'\omega)} + O(\omega^2)\,, \qquad (2)$$

i.e., $z_0 = (-\omega_0 + i\gamma)/Z_{\mathrm{CP}}$ and $z_1 = (1+i\gamma')/Z_{\mathrm{CP}}$. For the particle-hole symmetric case ω_0 and γ' are zero. We note that the in vicinity of $\omega = 0$ the local Green function $G(\omega)$ can thus be approximated by a simple pole. When neglecting γ', the parameter Z_{CP} equals the weight of the central peak of $A(\omega)$, which is approximated by a Lorentzian.

The parameters Z_{CP}, γ, ω_0, γ' are determined as follows. We employ the DMFT self-consistency equation

$$G(\omega) = G_0(\omega + \mu - \Sigma(\omega))\,,$$

which is equivalent to Eq. (1) [23]. Here

$$G_0(z) = \int d\epsilon\, \frac{\rho_0(\epsilon)}{z - \epsilon + i0}$$

is the propagator and $\rho_0(\omega)$ the density of states (DOS) for the noninteracting case. We also have the Fermi-liquid relations $\partial\Sigma/\partial\omega|_{\omega=0} = 1 - 1/Z_{\mathrm{FL}}$ and Luttinger's theorem [27], which reduces to $\mu - \Sigma(0) = \mu_0$ in DMFT, where μ_0 is the chemical potential for the corresponding noninteracting system. Altogether this leads us to the equations

$$z_0 = \frac{1}{G_0(\mu_0)}\,, \qquad z_1 = \frac{-G_0'(\mu_0)}{Z_{\mathrm{FL}} G_0(\mu_0)^2}\,,$$

which are immediately solved by taking real and imaginary parts, i.e.,

$$Z_{\mathrm{CP}} = \frac{1}{\mathrm{Re}\, z_1}\,, \qquad \gamma = \frac{\mathrm{Im}\, z_0}{\mathrm{Re}\, z_1}\,,$$
$$\omega_0 = \frac{-\mathrm{Re}\, z_0}{\mathrm{Re}\, z_1}\,, \qquad \gamma' = \frac{\mathrm{Im}\, z_0}{\mathrm{Re}\, z_1}\,.$$

The parameters Z_{CP}, γ, ω_0, γ' are thus determined by Z_{FL} and the bare DOS alone. For the parameters in Fig. 1 we obtain $Z_{\mathrm{CP}} = 0.135$, $\gamma = 0.076$ eV, $\omega_0 = 0$, $\gamma' = 0$.

Using the expansion (2), the first contribution to the self-energy [Eq. (1)] becomes

$$\mathrm{Re}[\omega + \mu - 1/G(\omega)] = \mathrm{const} + (1 - 1/Z_{\mathrm{CP}})\omega\,, \qquad (3)$$

i.e., this function is linear inside the central peak. On the other hand $\mathrm{Re}[\Delta(G(\omega))]$ is linear only on the narrower scale $|\omega| < |\omega_{\star,\pm}| \ll |\Omega_\pm|$ and is thus responsible for kinks in $\mathrm{Re}[\Sigma(\omega)]$ at $\omega_{\star,\pm}$, which are located inside the central peak. This location can now be calculated by inserting the linear ansatz for $1/G$ into $\Delta(G)$. To identify the relevant energy scales we proceed by expanding the DMFT self-consistency equation [23] as

$$\Delta(G) = (m_2 - m_1^2)G + (m_3 - 3m_1m_2 + 2m_1^3)G^2 + \cdots\,,$$

where m_i are the moments of the bare DOS. This moment expansion terminates after the first term for a semi-elliptical DOS; we omit the other terms in the following discussion. The kinks are located roughly at the extrema of $\mathrm{Re}[\Delta(G(\omega))]$, i.e., at

$$\omega_{\mathrm{max},\pm} = \omega_0 \pm \frac{\gamma + \gamma'\omega_0}{\sqrt{1+\gamma'^2}}\,. \qquad (4)$$

To better understand the energy scales involved we assume particle-hole symmetry for the moment and use the first-order expansion of $\Delta(G)$. Then we find

$$\omega_{\mathrm{max},\pm} \approx \pm\gamma \approx \pm 2qZ_{\mathrm{FL}}\sqrt{m_2 - m_1^2} =: Z_{\mathrm{FL}} D\,,$$

with $q = (p + 1/p)/2 \geq 1$ and $p = \pi\rho_0(\mu_0)\sqrt{m_2 - m_1^2}$. *The kink location is thus given by Z_{FL} times a non-interacting energy scale D which depends on the details of the DOS.* For example, for a half-filled band with semi-elliptical model DOS D is given by half the bandwidth.

An improved estimate of the kink energy scale $\omega_\star$ is obtained from the maximum curvature of $\mathrm{Re}[-\Delta(G(\omega))]$. The relevant solutions of $\partial^3\mathrm{Re}G/\partial\omega^3 = 0$ are

$$\omega_{\star,\pm} = \omega_0 \mp \frac{\gamma + \gamma'\omega_0}{\sqrt{1+\gamma'^2}}\left[1 - \sqrt{2}\left(1 \pm \frac{\gamma'}{\sqrt{1+\gamma'^2}}\right)^{1/2}\right]\,, \qquad (5)$$

which reduces to $\omega_\star = Z_{\mathrm{FL}}(\sqrt{2}-1)D$ for the particle-hole symmetric case. We obtain $\omega_\star = |\omega_{\star,\pm}| = 0.03$ eV for the parameters of Fig. 1. This agrees well with the location of the kinks in $\mathrm{Re}\Sigma(\omega)$, as seen in Fig. 2c, where $\pm\omega_\star$ is marked by blue circles.

Effective dispersion relation

For energies inside the central peak we now determine the effective dispersion $E_{\boldsymbol{k}}$, which is defined as the frequency ω) where $A(\boldsymbol{k}, \omega)$ has a maximum. Neglecting the ω dependence of $\mathrm{Im}\Sigma(\omega)$, kinks in $E_{\boldsymbol{k}}$ occur at the same energy $\omega_\star$ as the kinks in $\mathrm{Re}\Sigma(\omega)$. We approximate $\mathrm{Re}\Sigma(\omega)$ by a piecewise linear function with slope $1 - 1/Z_{\mathrm{FL}}$ inside the Fermi liquid regime and $1 - 1/Z_{\mathrm{CP}}$ in the intermediate-energy regime, i.e.,

$$\mathrm{Re}[\Sigma(\omega) - \Sigma(0)] = \begin{cases} a_- + (1 - 1/Z_{\mathrm{CP}})\omega & \text{for } \Omega_{\star,-} < \omega < \omega_{\star,-} \\ (1 - 1/Z_{\mathrm{FL}})\omega & \text{for } \omega_{\star,-} < \omega < \omega_{\star,+} \\ a_+ + (1 - 1/Z_{\mathrm{CP}})\omega & \text{for } \omega_{\star,+} < \omega < \Omega_{\star,+} \end{cases}\,. \qquad (6)$$

This approximation assumes that the self-energy constribution (3) dominates over $\mathrm{Re}[-\Delta(G(\omega))]$ outside the Fermi-liquid regime. Here $a_\pm = -(1/Z_{\mathrm{FL}} - 1/Z_{\mathrm{CP}})\omega_{\star,\pm}$ is required for continuity. We obtain the effective dispersion from the equation $E_{\boldsymbol{k}} + \mu - \epsilon_{\boldsymbol{k}} - \mathrm{Re}\Sigma(E_{\boldsymbol{k}}) = 0$ and use the approximation (6). This yields

$$E_{\boldsymbol{k}} = \begin{cases} Z_{\mathrm{CP}}(\epsilon_{\boldsymbol{k}} - \mu_0) + c_- & \text{for } \Omega_{\star,-} < E_{\boldsymbol{k}} < \omega_{\star,-} \\ Z_{\mathrm{FL}}(\epsilon_{\boldsymbol{k}} - \mu_0) & \text{for } \omega_{\star,-} < E_{\boldsymbol{k}} < \omega_{\star,+} \\ Z_{\mathrm{CP}}(\epsilon_{\boldsymbol{k}} - \mu_0) + c_+ & \text{for } \omega_{\star,+} < E_{\boldsymbol{k}} < \Omega_{\star,+} \end{cases} . \quad (7)$$

The effective dispersion thus follows the bare dispersion with two different renormalization factors: Z_{FL} in the Fermi liquid regime and Z_{CP} in the intermediate-energy regime. The offset in Eq. (7) is given by

$$c_\pm = Z_{\mathrm{CP}} a_\pm = -\left(\frac{Z_{\mathrm{CP}}}{Z_{\mathrm{FL}}} - 1\right)\omega_{\star,\pm} .$$

In the particle-hole symmetric case (half-filled band with symmetric DOS and $\mu_0 = 0$) we find the effective dispersions $E_{\boldsymbol{k}} = Z_{\mathrm{FL}}\epsilon_{\boldsymbol{k}}$ and $E_{\boldsymbol{k}} = Z_{\mathrm{CP}}\epsilon_{\boldsymbol{k}} \mp c$ with $c = |c_\pm|$, respectively. For the parameters in Fig. 1 we obtain $c = 0.018$ eV. As Fig. 1 shows, the agreement of these renormalized dispersions with the observed maxima of $A(\omega)$ is very good.

Further examples

We close with three figures in order to put the occurrence of electronic kinks into broader perspective.

A strongly correlated system *without particle-hole* symmetry is shown in Fig. 3. For this less than half-filled band we find a pronounced kink in the effective dispersion above the Fermi level. On the other hand, there is no kink below the Fermi level because the lower Hubbard band in $A(\omega)$ is not separated well enough from the central spectral peak.

For a degenerate *multi-band* system the analysis is very similar to that for a single-band system; results for $\mathrm{SrVO_3}$ (with three degenerate correlated bands) are given in Fig. 4.

Finally, Fig. 5 shows results for a *weakly correlated system* with particle-hole symmetry. For weakly correlated systems the spectral function $A(\omega)$ usually has a single peak, given by the bare DOS with additional broadening. The real part of the self-energy is much smaller than in the strongly correlated case and typically has a broad maximum near the lower and a minimum near the upper band edge. At these extrema the effective dispersion $E_{\boldsymbol{k}}$ crosses over from the FL dispersion $Z_{\mathrm{FL}}\epsilon_{\boldsymbol{k}}$ to the free dispersion $\epsilon_{\boldsymbol{k}}$, but the corresponding kinks are very faint since Z_{FL} is close to 1. Since $\mathrm{Re}[\omega - 1/G(\omega)]$ is approximately linear throughout the band, these weak kinks are located at the extrema of $\mathrm{Re}[-\Delta(G(\omega))] \approx -(m_2 - m_1^2)\mathrm{Re}[G(\omega)]$, i.e., at $\omega_{\mathrm{max},\pm}$ [Eq. (4)]. For the parameters of Fig. 5 we calculate ω_{max}=0.71 eV, which agrees well with the observed location of the crossover.

---

[1] A. Lanzara, P. V. Bogdanov, X. J. Zhou, S. A. Kellar, D. L. Feng, E. D. Lu, T. Yoshida, H. Eisaki, A. Fujimori, K. Kishio, J.-I. Shimoyama, T. Noda, S. Uchida, Z. Hussain, and Z.-X. Shen, Evidence for ubiquitous strong electron-phonon coupling in high-temperature superconductors, *Nature* **412**, 510 (2001).

[2] Z.-X. Shen, A. Lanzara, S. Ishihara, and N. Nagaosa, Role of the electron-phonon interaction in the strongly correlated cuprate superconductors, *Philos. Mag. B* **82**, 1349 (2002).

[3] H. He, Y. Sidis, P. Bourges, G. D. Gu, A. Ivanov, N. Koshizuka, B. Liang, C. T. Lin, L. P. Regnault, E. Schoenherr, and B. Keimer, Resonant Spin Excitation in an Overdoped High Temperature Superconductor, *Phys. Rev. Lett.* **86**, 1610 (2001).

[4] J. Hwang, T. Timusk, and G. D. Gu, High-transition-temperature superconductivity in the absence of the magnetic-resonance mode, *Nature* **427**, 714 (2004).

[5] M. Hengsberger, D. Purdie, P. Segovia, M. Garnier, and Y. Baer, Photoemission Study of a Strongly Coupled Electron-Phonon System, *Phys. Rev. Lett.* **83**, 592 (1999).

[6] T. Valla, A. V. Fedorov, P. D. Johnson, and S. L. Hulbert, Many-Body Effects in Angle-Resolved Photoemission: Quasiparticle Energy and Lifetime of a Mo(110) Surface State, *Phys. Rev. Lett.* **83**, 2085 (1999).

[7] E. Rotenberg, J. Schaefer, and S. D. Kevan, Coupling Between Adsorbate Vibrations and an Electronic Surface State, *Phys. Rev. Lett.* **84**, 2925 (2000).

[8] M. Higashiguchi, K. Shimada, K. Nishiura, X. Cui, H. Namatame, and M. Taniguchi, High-resolution angle-resolved photoemission study of Ni(1 1 0), *J. Electron Spectrosc. Relat. Phenom.* **144-147**, 639, (2005).

[9] J. Schäfer, D. Schrupp, E. Rotenberg, K. Rossnagel, H. Koh, P. Blaha, and R. Claessen, Electronic quasiparticle renormalization on the spin wave energy scale, *Phys. Rev. Lett.* **92**, 097205 (2004).

[10] A. Menzel, Zh. Zhang, M. Minca, Th. Loerting, C. Deisl, and E. Bertel, Correlation in low-dimensional electronic states on metal surface, *New J. Phys.* **7**, 102 (2005).

[11] H.-B. Yang, Z.-H. Pan, A. K. P. Sekharan, T. Sato, S. Souma, T. Takahashi, R. Jin, B. C. Sales, D. Mandrus, A. V. Fedorov, Z. Wang, and H. Ding, Fermi surface evolution and Luttinger theorem in $\mathrm{Na}_x\mathrm{CoO_2}$: a systematic photoemission study, *Phys. Rev. Lett.* **95**, 146401 (2005).

[12] Y. Aiura, Y. Yoshida, I. Hase, S. I. Ikeda, M. Higashiguchi, X. Y. Cui, K. Shimada, H. Namatame, M. Taniguchi, and H. Bando, Kink in the Dispersion of Layered Strontium Ruthenates, *Phys. Rev. Lett.* **93**, 117005 (2004).

[13] H. Iwasawa, Y. Aiura, T. Saitoh, I. Hase, S. I. Ikeda, Y. Yoshida, H. Bando, M. Higashiguchi, Y. Miura, X. Y. Cui, K. Shimada, H. Namatame, and M. Taniguchi, Orbital selectivity of the kink in the dispersion of $\mathrm{Sr_2RuO_4}$, cond-mat/0508312.

[14] Z. Sun, Y.-D. Chuang, A. V. Fedorov, J. F. Dou-

glas, D. Reznik, F. Weber, N. Aliouane, D. N. Argyriou, H. Zheng, J. F. Mitchell, T. Kimura, Y. Tokura, A. Revcolevschi, and D. S. Dessau, Quasiparticle-like peaks, kinks, and electron-phonon coupling at the (π,0) regions in the CMR oxide $La_{2-2x}Sr_{1+2x}Mn_2O_7$, cond-mat/0510255.

[15] F. Ronning, T. Sasagawa, Y. Kohsaka, K. M. Shen, A. Damascelli, C. Kim, T. Yoshida, N. P. Armitage, D. H. Lu, D. L. Feng, L. L. Miller, H. Takagi, and Z.-X. Shen, Evolution of a metal to insulator transition in $Ca_{2-x}Na_xCuO_2Cl_2$ as seen by angle-resolved photoemission, *Phys. Rev. B* **67**, 165101 (2003).

[16] T. Yoshida, K. Tanaka, H. Yagi, A. Ino, H. Eisaki, A. Fujimori, and Z.-X. Shen, Direct observation of the mass renormalization in $SrVO_3$ by angle resolved photoemission spectroscopy, *Phys. Rev. Lett.* **95**, 146404 (2005).

[17] J. Graf, G.-H. Gweon, K. McElroy, S. Y. Zhou, C. Jozwiak, E. Rotenberg, A. Bill, T. Sasagawa, H. Eisaki, S. Uchida, H. Takagi, D.-H. Lee, and A. Lanzara, Universal high energy anomaly in the electron spectrum of high temperature superconductors by angle-resolved photoemission spectroscopy, cond-mat/0607319.

[18] A. A. Abrikosov, L. P. Gorkov, and I. E. Dzyaloshinski, Methods of Quantum Field Theory in Statistical Physics, Dover Publications (New York, 1975).

[19] W. Metzner and D. Vollhardt, Correlated Lattice Fermions in $d = \infty$ Dimensions, *Phys. Rev. Lett.* **62**, 324 (1989).

[20] Th. Pruschke, M. Jarrell, J. K. Freericks, Anomalous normal-state properties of high-T_c superconductors: intrinsic properties of strongly correlated electron systems? *Adv. Phys.* **44**, 187 (1995).

[21] A. Georges, G. Kotliar, W. Krauth, and M. J. Rozenberg, Dynamical mean-field theory of strongly correlated fermion systems and the limit of infinite dimensions, *Rev. Mod. Phys.* **68**, 13 (1996).

[22] G. Kotliar and D. Vollhardt, Strongly Correlated Materials: Insights from Dynamical Mean-Field Theory, *Physics Today* **57**, 53 (2004).

[23] In DMFT, $\Delta(G)$ is determined by the requirement $G(\omega) = G_0(\omega + \mu - \Sigma(\omega))$, i.e., $G_0(\Delta(G) + 1/G) = G$. Here $G_0(\omega)$ is the local Green function in the absence of interactions.

[24] I. A. Nekrasov, K. Held, G. Keller, D. E. Kondakov, Th. Pruschke, M. Kollar, O. K. Andersen, V. I. Anisimov, and D. Vollhardt, Momentum-resolved spectral functions of $SrVO_3$ calculated by LDA+DMFT, *Phys. Rev. B* **73**, 155112 (2006).

[25] R. Bulla, Th. Pruschke, and A. C. Hewson, Metal-insulator transition in the Hubbard model, *Physica B* **259-261**, 721 (1999).

[26] The mechanism discussed here applies to systems with localized d or f-orbitals, where the local interaction between electrons is dominant. The long-range part of the interaction is viewed on a mean-field level as in a local-density approximation theory for band structure calculations.

[27] E. Müller-Hartmann, The Hubbard model at high dimensions: some exact results and weak coupling theory, *Z. Phys. B* **76**, 211 (1989).

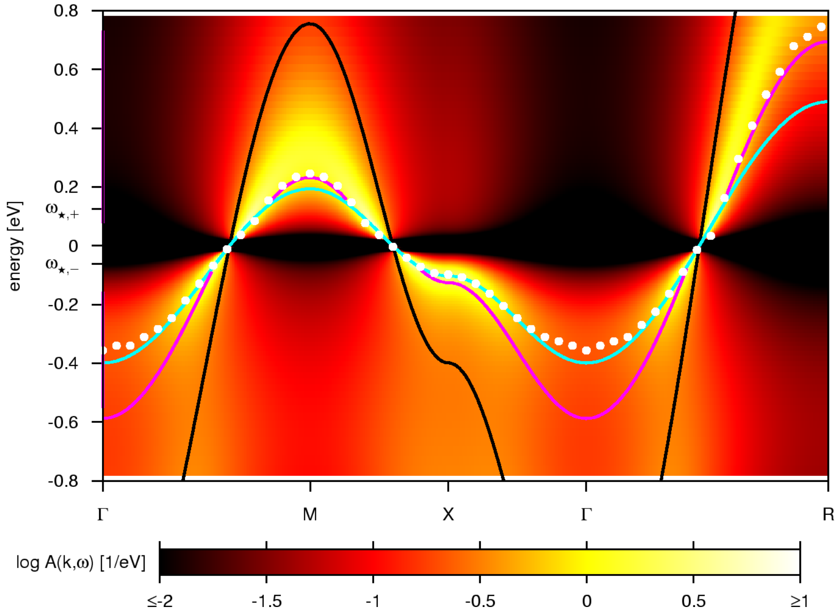

FIG. 3: Intensity plot of the spectral function $A(\boldsymbol{k},\omega)$ for a strongly correlated system without particle-hole symmetry (Hubbard model in DMFT, cubic lattice, U=4 eV, bandwidth $W = 3.46$ eV, n=0.8, Z_{FL}=0.26). The effective dispersion $E_{\boldsymbol{k}}$ (white dots) follows $Z_{\mathrm{FL}}\epsilon_{\boldsymbol{k}}$ (blue line) near the Fermi level. At $\omega_{\star,+}$=0.062 eV it crosses over to $Z_{\mathrm{CP}}\epsilon_{\boldsymbol{k}} + c_+$ (pink line at positive energies, $Z_{\mathrm{CP}} = 0.40$, c_+=0.035 eV). The crossover between these two regimes leads to a pronounced kink. Here $\omega_\star$, Z_{CP}, and c_+ were calculated from Z_{FL} and the uncorrelated band structure as described above. On the other hand, below the Fermi level there is no crossover to $Z_{\mathrm{CP}}\epsilon_{\boldsymbol{k}} + c_-$ (pink line at negative energies) because the lower Hubbard subband is not separated well enough from the central spectral peak.

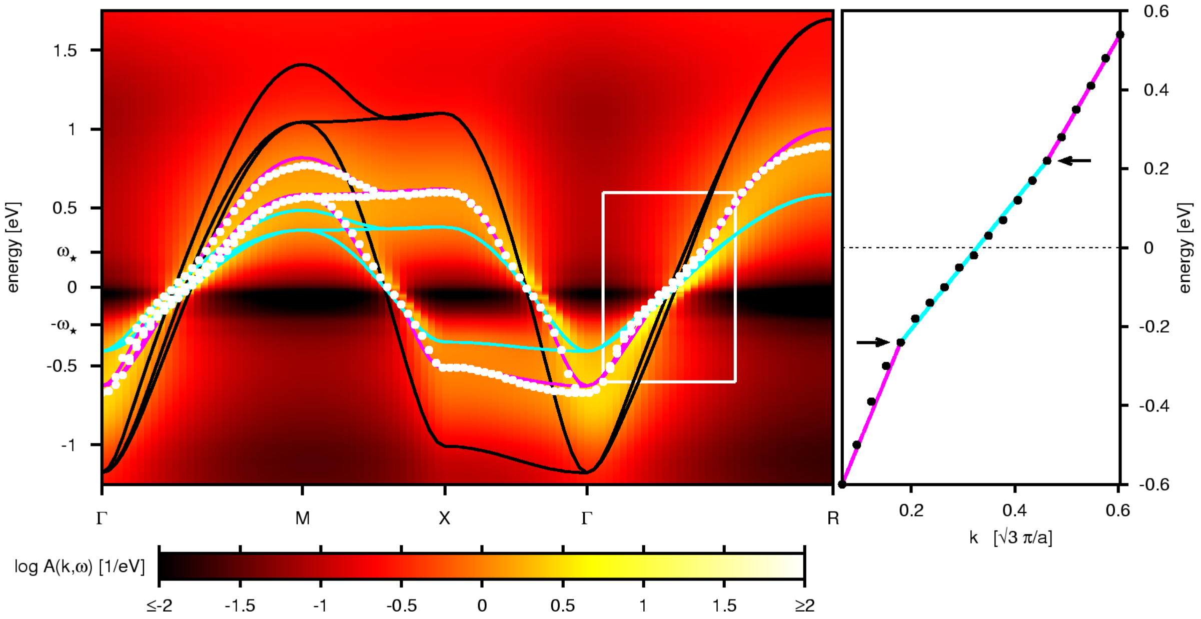

FIG. 4: Kinks in the dispersion relation $E_{n\boldsymbol{k}}$ (white dots) obtained for SrVO$_3$ with LDA+DMFT. In the vicinity of the Fermi energy it follows the LDA band structure $\epsilon_{n\boldsymbol{k}}$ (black lines) renormalized by a Fermi-liquid factor $Z_{\text{FL}} = 0.35$, i.e. $E_{n\boldsymbol{k}} = Z_{\text{FL}}\epsilon_{n\boldsymbol{k}}$ (blue line). Outside the Fermi-liquid regime the dispersion relation follows the LDA band structure with a different renormalization, $E_{n\boldsymbol{k}} = Z_{\text{CP}}\epsilon_{n\boldsymbol{k}} + c_\pm$ (pink line), with $Z_{\text{CP}} = 0.64$, c_+=0.086 eV, c_- =0.13 eV (as determined from the linear approximation to $1/G$, in contrast to [24]). Along the directions Γ-M and Γ-R the crossover between the two regimes leads to kinks at energies $\omega_{\star,+}$=0.22 eV and $\omega_{\star,-}$=-0.24 eV in the effective dispersion. These kinks are marked by arrows in the plot on the right, which corresponds to the white frame and shows the approximately piecewise linear dispersion of the lowest-lying band. From the intensity plot of the spectral function $A(\boldsymbol{k},\omega)$ we note that in the intermediate-energy regime the resonance is rather broad but nonetheless dispersive. The LDA+DMFT calculation was performed for Hubbard interaction $U = 5.55$ eV and exchange interaction $J = 1.0$ eV [24]; due to the degeneracy of the t_{2g} band the self-energy obtained from DMFT is a diagonal matrix with equal elements. The results were obtained at temperature $T = 0.1$ eV with QMC as the impurity solver.

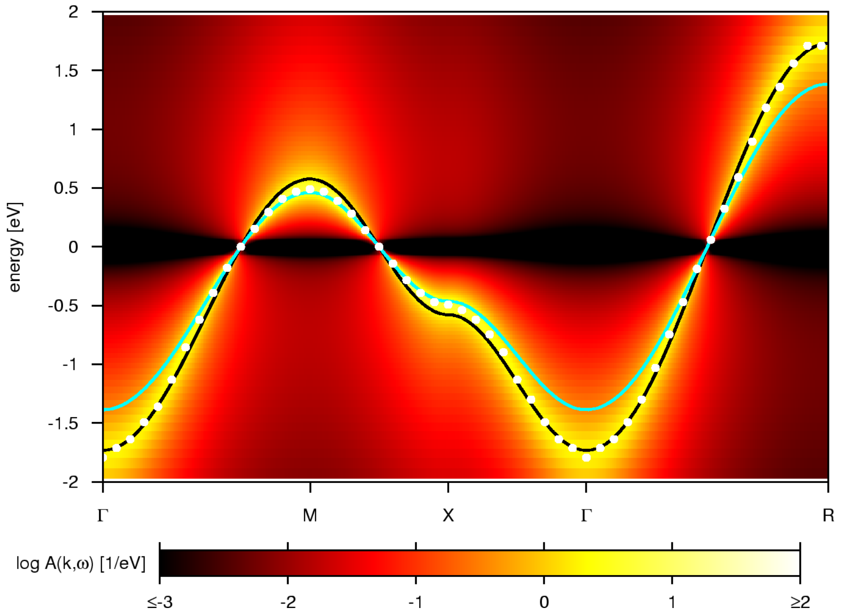

FIG. 5: Intensity plot of the spectral function $A(\boldsymbol{k},\omega)$ for a weakly correlated system (Hubbard model in DMFT, cubic lattice, U=1 eV, bandwidth $W = 3.46$ eV, n=1, Z_{FL}=0.80). The effective dispersion $E_{\boldsymbol{k}}$ (white dots) follows $Z_{\text{FL}}\epsilon_{\boldsymbol{k}}$ (blue line) near the Fermi level and crosses over to bare dispersion $\epsilon_{\boldsymbol{k}}$ (black line) at higher energies. The crossover between these two regimes does not lead to a sharp kink. As in Fig. 1, the Gaussian DOS for the hypercubic lattice with t_*=1 eV was used, which for a three-dimensional cubic lattice corresponds to $t = t^*/\sqrt{6}$, i.e., bandwidth $W = 3.46$ eV.